

Study on Base Station Topology in National Cellular Networks: Take Advantage of Alpha Shapes, Betti Numbers, and Euler Characteristics

Ying Chen¹, Rongpeng Li¹, Zhifeng Zhao¹, and Honggang Zhang¹

Abstract—Faced with the ever-increasing trend of the cellular network scale, how to quantitatively evaluate the effectiveness of the large-scale deployment of base stations (BSs) has become a challenging topic. To this end, a deeper understanding of the cellular network topology is of fundamental significance to be achieved. In this paper, α -Shape, a powerful algebraic geometric tool, is integrated into the analyses of real BS location data for six Asian and six European countries. First, the BS spatial deployments of both Asian and European countries express fractal features based on two different testifying metrics, namely the Betti numbers and the Hurst coefficients. Second, it is found out that the log-normal distribution presents the best match to the cellular network topology when the practical BS deployment is characterized by the Euler characteristics.

Index Terms—Base stations, mobile communication, network topology, wireless communication.

I. INTRODUCTION

A. Motivations

RECENTLY, driven by the explosive installment of base stations (BSs) globally, the issue of the optimal BS deployment, i.e., a collection of BSs distributed on the two-dimensional (2-D) plane [1], of cellular networks has attracted tremendous concern from both academic and industrial communities. Indeed, just as the name of “cellular” has been coined 40 years ago, the BSs were assumed to be deployed based on the well-known 2-D hexagonal grid model in the initial stages. Such an assumption leads to obvious fractal phenomenon in a pure geometric pattern. However, together with the continuous long-term evolutions of cellular networks in the past several decades, diverse configurations of BSs have been springing up to meet various application requirements, such as microcell cellular networks, femtocell cellular networks, ultra-dense cellular networks, etc.

Manuscript received December 17, 2018; revised March 4, 2019; accepted May 20, 2019. Date of publication June 21, 2019; date of current version June 3, 2020. This work was supported in part by National Key R&D Program of China under Grant 2017YFB1301003, in part by the National Natural Science Foundation of China under Grants 61701439 and 61731002, in part by the Zhejiang Key Research and Development Plan under Grants 2019C01002 and 2019C03131, and in part by the Fundamental Research Funds for the Central Universities. (Corresponding author: Rongpeng Li.)

The authors are with the College of Information Science and Electronic Engineering, Zhejiang University, Hangzhou 310027, China (e-mail: 21631088chen_ying@zju.edu.cn; lirongpeng@zju.edu.cn; zhaofz@zju.edu.cn; honggangzhang@zju.edu.cn).

Digital Object Identifier 10.1109/JSYST.2019.2920658

The overlapping and coexistence of heterogeneous BS deployments has gradually made the original geometric fractal property ambiguous or even invisible. Under these complicated circumstances, more accurate understandings of the BS deployments are of great significance to enhance the studies on cellular networks.

Admittedly, the BS deployments have been changing over decades due to the emergence of various network standards (2G/3G/4G/5G) and technologies. In this regard, powerful algebraic geometric tools, namely α -Shapes, Betti numbers, and Euler characteristics [2]–[4] are selected in this paper to study the topological features in national cellular networks for reasons as follows.

- 1) First, in the algebraic geometry field, α -Shapes, Betti numbers, and Euler characteristics are widely used in the topological analyses of manifolds. From the theoretic point of view, the algebraic geometry tools (α -Shape modeling) [2] adopted in this paper are very robust to the variances of network dynamics (including large-scale BS deployments). Moreover, the Betti numbers and Euler characteristics [3], which are also referred to as persistent homology in algebraic geometry, are born to reflect the intrinsically invariant topological features in a complex discrete point set regardless of any concrete changes in its spatial distributions.
- 2) Second, these algebraic geometry tools have been widely applied in much more complicated scenarios including wireless networking scenarios. Some representative examples are mentioned below.
 - a) α -Shapes and Betti numbers have already been incorporated in investigating and modeling the cosmic web [3], [4]. In particular, it has been verified that Betti numbers can be exploited to measure the hierarchical cosmos evolution, as well as the dark energy nature, in astronomical observations. As we know, astronomical planets under constant evolutions are extremely far away from the observation stations on the earth. Limited by the existing measurement methods and apparatus, measuring errors or deviations are inevitable in the collected data to some extent. Even so, these tools still succeeded in revealing the fundamental topological features in the ever-evolving cosmic web in [3]. Similarly, the long-term evolution of cellular mobile networks has

been undergoing a long period of more than 40 years from 1G, 2G, 3G, 4G to 5G. The cellular mobile networks have already become extremely complicated, with huge dimension of various parameters, heterogeneous architectures, millions of BSs of different types (macrocells, microcells, femtocells, small-cells, etc.) at the national level, and coverage densification to personal area networking. Therefore, in order to grasp the intrinsically fundamental features and patterns of the evolution of the next-generation (future) mobile cellular networks, α -Shapes, Betti numbers, and Euler characteristics will surely play significant roles as in cosmic web.

- b) Betti numbers, or so-called persistent homology, have provided an alternative perspective for coverage problems in wireless sensor networks (WSNs) [5]. By leveraging persistent homology theory, [5] has proven that, regardless of topological types, a stationary set of sensors is capable of guaranteeing coverage in a bounded region.

As a matter of fact, in addition to the study on BS topology based on large-scale countries [6], we also push our study forward to the urban scale, and the topological findings in urban cellular networks have been included in [7]. Basically, it is indispensable to investigate national and urban BS topology issues separately. As we know, the same rules hold for the whole system are not necessarily correct for a part of the complex system based on the complex system theory, and vice versa. On the other hand, the BS topological features in national and urban cellular networks are uniquely meaningful from both theoretical and application views.

To sum up, it is significant and intriguing to incorporate the algebraic geometric tools, namely α -Shapes, Betti numbers, and Euler characteristics, into the topological analyses of BS deployments in cellular networks.

B. Related Works

In order to meet various performance requirements, substantial efforts have been made on how to effectively address the cellular network deployment issues. Ericson [8] investigated the influence of cell size on the network energy consumption for the purpose of maximizing energy efficiency. In [9], an optimal approach was presented to prolong the lifetime of WSNs by deploying BSs appropriately. Stochastic geometry models were built in [1] for BS deployments in shared cellular networks, and the proposed models were observed to be suitable for different countries. Liu *et al.* [10] proposed to jointly optimize the placement of BSs with other factors like power control. Wu and Niu [11] studied the BS deployment scheme based on the overall traffic variation process rather than the peak traffic load, which can successfully bring energy consumption reduction and performance improvement. Coskun and Ayanoglu [12] developed a greedy framework to arrange the BSs in heterogeneous cellular networks, so as to improve the energy efficiency. In the strive for meeting coverage demands and traffic requirements, the BSs were automatically planned and distributed in [13] in mobile

networks. From an energy reduction perspective, Mahmud *et al.* [14] proposed a heuristic method to lay out the BSs in the WSNs.

Undoubtedly, the knowledge of topology of the cellular networks is extremely beneficial for the guidance on BS deployments. Since the locations of BSs are of paramount importance in determining the network topology, a range of researches on the spatial distribution of BSs have been carried out in recent decades. In [15], the severe divergence of Poisson distribution from practical BS density distribution was found out, and α -stable distribution, one of the heavy-tailed distributions, was shown to match the real distribution more properly. By separating the BSs into diverse subsets, a comprehensive study on the cellular network's spatial structure was presented in [16], and the clustering feature of BS density distribution was also revealed. In [17], further study about the strong linear dependence was exhibited between BS deployment and spatial traffic distribution. Taking different scenarios into account, Chiaraviglio *et al.* [18] claimed that the log-normal and Weibull distributions were the more precise ones to fit the real BS deployments in rural and coastal scenarios, respectively. Zhao *et al.* [19] verified the validity of α -stable distribution for the temporal traffic series in addition to the spatial density of BSs.

Understanding the network topology can prominently facilitate the design of efficient cellular networks, and pervasive applications depending upon the network topology have been found in the wireless communication field. For instance, the knowledge of network topology can be exploited to perform automatic computations for topology control in WSNs [20], investigate the pros and cons of BS switching ON/OFF scheme [21], develop energy-saving mechanism for green cellular networks [22], improve the spectral efficiency and reduce the bit error rate in space-time network coding scheme [23], manage the interference and allocate spectrum resource for a femtocell-based cellular network [24], etc.

C. Our Contributions

Most of the previous literatures analyzed the cellular network deployments from the perspective of BS spatial density distribution by straightforward simulation methods. As one of the unprecedented researches, this paper introduces a powerful algebraic geometric tool, namely α -Shapes [4], into the fundamental analyses of real BS location data for 12 countries around the world, and generalizes essential topological characteristics through the mass datasets from the perspective of topological invariants, i.e., Betti numbers and Euler characteristics [4]. Briefly speaking, BSs can be abstracted into a collection of points, and α -Shapes are geometric manifolds constructed from a specific point set so that they are closely related to topological nature of the point set. Moreover, the Betti numbers and the Euler characteristics can be used to describe the topological information in the α -Shapes, thus also tightly associated with the topological features of the point set, or the BSs in this paper.

Specifically, our works aim to answer this kind of question: Is there any essentially identical features hidden in the network topology regardless of the geographical differences and temporal evolutions? In other words, it is an interesting and profound

issue to find out the topological features in the cellular network topology. In this regard, the main contributions of this paper are as follows.

- 1) First of all, the fractal phenomenon is revealed in the BS spatial deployments for both Asian and European countries in terms of the Betti numbers and the Hurst coefficients.
- 2) Second, it is verified that log-normal distribution provides the most conforming fitness with the cellular network topology when the practical BS deployments are characterized by the Euler characteristics.

In fact, fractal characteristics in the BS deployments have been applied in a plenty of works for the study of cellular networks. Below are some typical examples.

One prominent advantage of fractal features is that it could facilitate more sophisticated stochastic geometry models of cellular networks [25]. By leveraging the essences of fractal property, i.e., self-similarity, in the spatial deployments of BSs, it has been found that the BS deployments could be more easily analyzed in a large-scale area [25].

On the other hand, fractal features can be embedded into the performance evaluation of cellular networks [25], [26]. For instance in [25], based on the self-similarity among BSs, a tractable solution for the coverage probability in a large-scale area has been deduced. In particular, an upper bound of the derived coverage probability for high signal-to-interference-plus-noise ratio (SINR) thresholds has been given in [25]. Second, motivated by the fractal coverage characteristics, the average achievable rate and the area spectral efficiency have been re-evaluated for fractal small cell networks in [26].

More interestingly, in addition to the fractal phenomenon, we have also verified a completely valuable discovery, i.e., the fitness of log-normal distribution for the cellular network topology when the practical BS deployments in either European or Asian countries are characterized by the Euler characteristics, and we believe it will provide fruitful guidance on the analysis and design of BS deployments in the future, such as providing diverse network performance metrics, improving the models of spatial patterns of BS deployments, etc.

In summary, we believe that our contributions in this paper have substantial potentials to reduce the analytical gap between existing models and the realistic spatial BS deployments, thus laying the foundation to bring enlightenments to in-depth studies on BS topology. In addition, it could contribute to the performance examinations under more complicated network scenarios and enhance theoretical comprehensions of the actual network variations.

This paper is organized as follows. The vital algebraic topological invariants and tools, including α -Shapes, Betti numbers, and Euler characteristics, are introduced in Section II. The detailed description for the cellular network data is given in Section III. The fractal features of BS deployments in Asian and European countries are clarified in Section IV. The identical log-normal distribution of the Euler characteristics for the above-mentioned countries is illustrated in Section V. Finally, conclusions are drawn in Section VI.

Moreover, in order to improve the readability of this paper, the notations involved and their meanings are listed in Table I.

TABLE I
NOTATIONS AND THEIR MEANINGS IN THIS PAPER

Notations	Meanings
α	The scale parameter in α -shapes.
\mathbf{S}	A two-dimensional point set.
\mathbf{A}	Another two-dimensional point set.
β_0	The number of connected objects or points.
β_1	The number of tunnels in a manifold.
χ	The Euler characteristic.
\mathbf{O}	A 3-dimensional object.
$\partial\mathbf{O}$	The boundary of \mathbf{O} .
x	A point in the surface of \mathbf{O} .
$R_1(x), R_2(x)$	The principal radius of the curvature at the point x .
H	The Hurst coefficient.

II. FUNDAMENTAL TOOLS FOR TOPOLOGY DISCOVERY

In this section, the principal concepts of the algebraic topological tools used for topology discovery in our works are presented. Various information in all aspects about these tools will be provided, including the basic definitions, the relevant applications, the constructions, etc. The relationships between them will also be expounded.

A. Alpha Shapes (α -Shapes)

As one of the most fundamental notions from the domain of computational topology in algebraic geometry [27], [28], α -Shapes were first introduced by Knuth [29]. α -Shapes have been extensively applied to a plenty of vital domains. Typical examples of the applications based on α -Shapes modeling include: protein-DNA interactions can be precisely predicted [30], molecular shapes can be described in detail [31], properties of macro-molecular can be analytically exacted [32] in the field of biology; interactions between the origin and destinations can be summarized and visualized in geography [33]; network edges can be detected locally in ad hoc networks [34]; surface morphology of products can be analyzed in manufacturing. Applications in other fields include shape similarity comparisons of 3-D models [35], medical image analyses and so forth.

In general, unlike common tools in algebraic topology field, which have to resort to some kind of user-defined smoothing functions or thresholds for the analyses of a discrete point set, α -Shapes depend entirely on the point set itself, and focus on the features determined by the set of points exclusively [4]. In this regard, α -Shapes are significantly superior and are regarded as the optimal technique for this paper.

In an informal definition, α -Shapes can be considered as the intuitive notion of the shape of a specific discrete point set [36]. For example, without loss of generality, a point set \mathbf{S} and one of its α -Shapes are illustrated in Fig. 1. As shown in Fig. 1, the α -Shape is in accordance with our intuition about the shape of \mathbf{S} . In addition, the processes of construction will be elaborated later in this section.

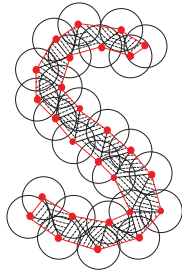


Fig. 1. Point set S and one of its α -Shapes. The point set S is represented by the red nodes in the 2-D plane, and the α -Shape of S is denoted by the red outline of the area with black dotted shadows. In addition, the black circles and edges between nodes include the intermediate results during the construction of α -Shapes.

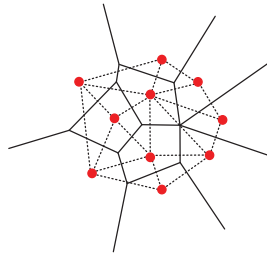


Fig. 2. Voronoi tessellation and the Delaunay triangulation of A , where the red nodes belong to the point set A , the dotted lines refer to the Delaunay triangulation, and the solid lines indicate the edges of the Voronoi tessellation.

Two topological concepts closely related to the construction of α -Shapes are the Voronoi tessellation and the Delaunay triangulation. Let a 2-D point set A , a subset of the 2-D real number point set \mathbf{R}^2 , consist of node a_i ($i = 1, 2, \dots, n$), where n is the total number of A . Then, a Voronoi cell V_i refers to the set of points that are closer to a_i than any other nodes in A , as expressed in the following equation, and the Voronoi diagram of A is composed of the set of Voronoi cells [36]:

$$V_i = \{x \in \mathbf{R}^2 \mid \|x - a_i\| \leq \|x - a_j\|, \forall j = 1, 2, \dots, n, j \neq i\}. \quad (1)$$

The Delaunay triangulation is coupled with the Voronoi tessellation. An edge connecting two nodes belongs to the Delaunay triangulation if and only if the two corresponding Voronoi cells share a common side. Similarly, a triangle connecting three nodes belongs to the Delaunay triangulation if and only if the three corresponding Voronoi cells share a common corner [36]. The Voronoi tessellation and the Delaunay triangulation of A are depicted as Fig. 2.

Fig. 3 represents the process of one α -Shape construction given the scale parameter α . Specifically, here follows the outline of building up α -Shapes. First, the Voronoi tessellation and the Delaunay triangulation of the point set A are obtained in Fig. 3(a). Second, taking the scale parameter α as the radius, circles centered by every point in A are drawn. Then, the set of circles forms the area $C(\alpha)$, as shown by the pink area in Fig. 3(b), in which the straight lines indicate the edges of the Voronoi tessellation. Third, the alpha complex consists of the simplexes, namely the vertexes, edges, and triangles, which are

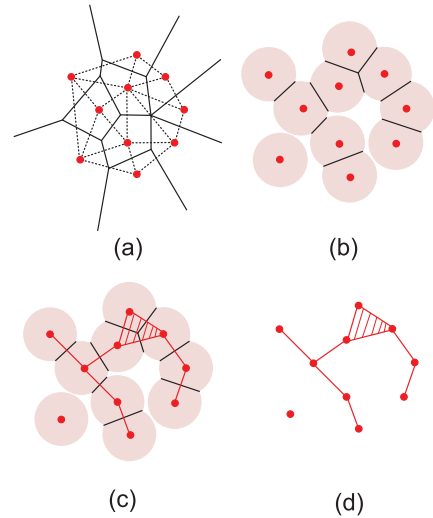


Fig. 3. Illustration of α -Shapes construction.

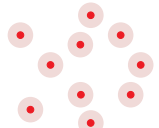
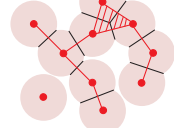


		
	(a)	(b)
β_0	10	2
β_1	0	0
		
	(c)	(d)
β_0	1	1
β_1	1	0

Fig. 4. Features of α -Shapes as α , i.e., the radius of the pink circles in each subgraph, increases gradually from zero to infinity.

entirely included in the area $C(\alpha)$, as displayed by the red part in Fig. 3(c). Finally, one α -Shape is obtained in Fig. 3(d).

The features of α -Shapes demonstrate themselves when α increases gradually from zero to infinity, as shown in Fig. 4. The α -Shape is equivalent to the point set itself when α is equal to zero. Then, a new Delaunay simplex is added into the α -Shapes when α exceeds some threshold, which means the α -Shapes vary by the values of α in a discrete manner. So alpha complex is the same as the Delaunay triangulation of A when α reaches some maximum value α_{max} , and the α -Shape keeps being the convex hull of A afterward. Therefore, the number of α -Shapes is actually finite although the scale parameter α varies from 0 to $+\infty$.

In summary, α -Shapes are the intuitive description of point sets, the subsets of the Delaunay triangulation, and the generation of the convex hull.

B. Betti Numbers

The basic notion of homology needs to be stated first for a better elaboration of the Betti numbers. Homology describes the connectivity of space via the characterization of two fundamental morphological elements, namely holes and boundaries [2]. In terms of 3-D space, a 0-D hole refers to an independent component or a gap between two disconnected components; a 1-D hole means a tunnel that appears when an edge is added to two connected points, and the tunnel can be crossed over in either direction without running into a boundary; a 2-D hole is a cavity or void, which is completely encircled by a 2-D surface. Boundaries are usually described by cycles. A 0-cycle indicates a connected object or a point; a closed loop is identified as a 1-cycle; whereas a 2-D surface is referred to as a 2-cycle. The p th homology group H_p is composed of all p -D holes or cycles [3].

The p th Betti number β_p can be seen as the number of elements in the p th homology H_p . As a result, the Betti numbers contain complete topological information about a space. Similar as the p th hole, β_0 is the number of independent components of a space; β_1 means the number of independent tunnels; β_2 indicates the number of independent enclosed voids [3].

The Betti numbers can be inferred from α -Shapes in a straightforward way. As illustrated in Fig. 4, the α -Shapes evolve from the point set itself into the Delaunay triangulation gradually as the growth of the scale parameter α . In other words, the set of α -Shapes is actually a filtration of the Delaunay triangulation, where α plays the role of filtration parameter [37]. Therefore, each Betti number can be expressed as a function of α since every α -Shape corresponds to certain values of the Betti numbers as listed in Fig. 4 for the enhancement of understanding.

C. Euler Characteristics

The Euler characteristic is one of the most principle concepts in analyzing the topology of a space, especially in capturing the global features and statistical characteristics.

Let \mathbf{O} be a 3-D object whose boundary $\partial\mathbf{O}$ is a 2-D enclosed shell. In the formal definition, the Euler characteristic $\chi(\partial\mathbf{O})$ is equal to the integrated Gaussian curvature of the surface [4] as

$$\chi(\partial\mathbf{O}) = \frac{1}{2\pi} \oint_x \frac{dx}{R_1(x)R_2(x)} \quad (2)$$

where $R_1(x)$ and $R_2(x)$ are two principal radii of the curvature at the point x of the shell. Surprisingly, the integration mentioned above remains invariant under continuous deformation of the surface [4], which is the reason why the Euler characteristic can reflect the essential property of a space and is referred to as a topological invariant.

According to the Euler–Poincaré Formula, the Euler characteristic can also be obtained by the Betti numbers [4]. Specifically, the Euler characteristic is equal to the alternating sum of the Betti numbers [4] as

$$\chi = \beta_0 - \beta_1 + \beta_2 - \beta_3 + \dots \quad (3)$$

TABLE II
BASIC INFORMATION OF 12 SELECTED COUNTRIES

Country	Area(/km ²)	No. of BSs	Density of BSs(1/km ²)	
Europe	Poland	312685	136905	0.4378
	UK	244100	160827	0.6589
	Germany	357376	276408	0.7734
	France	553965	273279	0.4933
	Italy	301338	180867	0.6002
	Netherlands	41864	83891	2.0040
Asia	Singapore	719.1	13396	18.6288
	South Korea	100210	38845	0.3876
	Japan	377972	316977	0.8386
	China	9634057	193764	0.0201
	Tailand	513120	62410	0.1216
	India	2980000	178834	0.0600

In this paper, only two Betti numbers β_0 and β_1 are taken into account since the 2-D location data of BSs in the cellular networks are analyzed.

III. DATASET DESCRIPTION

In order to achieve precise and effective topological characterizations, our works are based on the analyses of a rich supply of mass data gained from *OpenCellID* community, an open-source data platform for providing the locations of BSs in various countries around the world (<https://community.opencellid.org/>) [38]. The massive BS data of 12 countries, including six representative countries from Asia and Europe, respectively, have been extracted from the *OpenCellID* dataset. Each information entry consists of the location of BSs, namely the latitude and longitude data, and other auxiliary information. The basic information about the 12 selected countries is listed in Table II, including the territory area, the total number, and the average density of BSs.

To express the reliability of the extracted data, the latitude and longitude data are converted into the location data on a 2-D coordination system in the form of x and y , and the BS deployment diagrams of several representative countries, including three Asian countries and three European ones, are illustrated in Fig. 5. The red boundary lines are extracted from the Google Map, and it is observed that the layout formed by the BSs is basically the same as the real territory configuration since almost all the BS data fall within the boundary line of each country.

IV. FRACTAL NATURE IN THE CELLULAR NETWORKS TOPOLOGY

As a fundamental feature of networks, fractal phenomenon has been found in a number of wireless networking scenarios [39]. For instance, the design of hand-off scheme for mobile terminals can be inspired by the fractal property [40], and a fractal shape demonstrates itself in the coverage boundary of

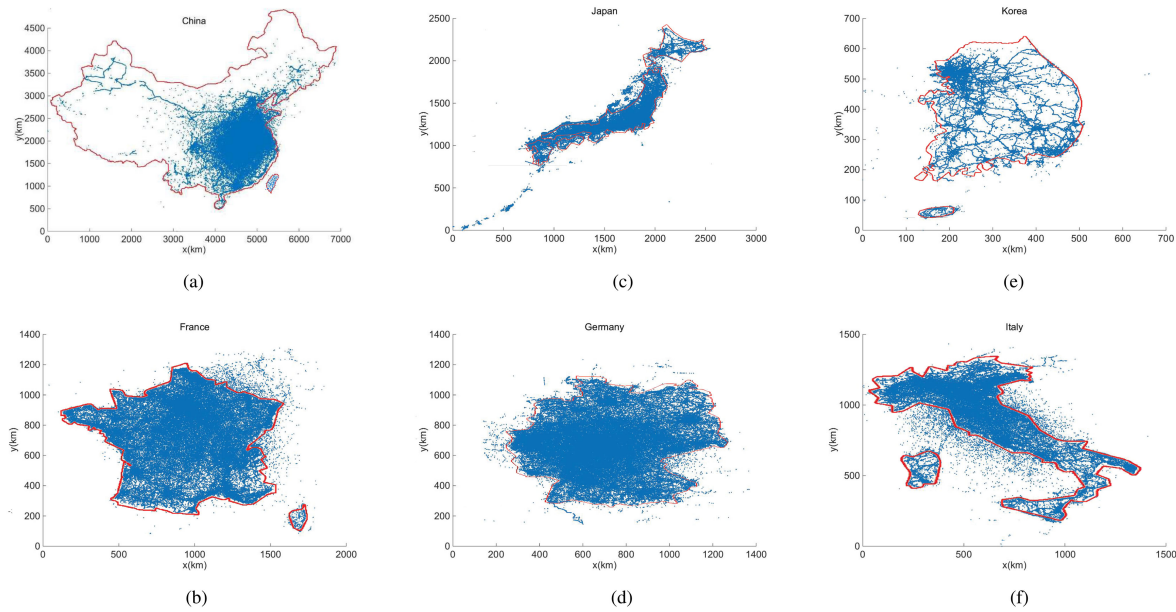


Fig. 5. BS deployment diagrams of three (upper) Asian and (lower) European countries. (a) China. (b) France. (c) Japan. (d) Germany. (e) South Korea. (f) Italy.

the wireless cellular network [41]. Moreover, a rich number of networks in the real world exhibit the significant fractal characteristics naturally, such as the worldwide web, yeast interaction, protein homology, and social networks [42], [43]. Based on the tools of α -Shapes, Betti numbers, and Hurst coefficients, this section confirms the fractal nature in cellular networks from the perspective of the topology of BSs [3].

A. Comparisons Between the Betti Curves of Fractal and Random Point Distributions

Fig. 6 gives intuitive comparisons between the Betti curves brought by the random characteristics and the fractal patterns.

Fig. 6(a) expresses the practical point deployments for the random and fractal cases. One of the most significant features of fractal behavior is the self-similarity under any length scale [44], and self-similarity is added into the point distribution by the hierarchical partitions of the area among the points, while the random point distribution is simply realized by the random choice of the location for each point.

Fig. 6(b) shows the Betti curves for the random case, whereas Fig. 6(c) for the fractal case. The β_0 curve for the random case demonstrates a trend of descending monotonously, and the β_1 curve presents a single peak formed by the monotone decrease after the monotone rise of β_1 . However, in the fractal case, distinctive from the random case, the β_0 curve manifests itself by the multiple ripples in the global decline trend, where a ripple is characterized by the rapid slope switch within a narrow range of α , as shown by the amplified blue subgraph in the left window in Fig. 6(c). In the meantime, the β_1 curve for the fractal case fluctuates in the form of multiple peaks. In other words, the fractal behavior brings the distinguishing features of multiple ripples and peaks into the β_0 and β_1 curves, respectively [3]. In addition, the identical number of ripples and peaks is an indication for the hierarchical levels in the fractal distribution

[3]. For example, the first two levels, out of the total three levels in the fractal distribution, demonstrate themselves in a visible way by the two ripples or peaks in the Betti curves, while the last level is not observed clearly in the curves because of the trivial number of elements in this level. Moreover, the ripples arrive prior to the corresponding peaks, which is quite reasonable because the size of components is smaller than that of loops.

B. Fractal Features in Terms of the Betti Numbers

Within our works, the fractal phenomenon in the cellular networks is discovered based on the modularity patterns (structures hierarchy) of the Betti curves of the practical BS distributions [3], as verified in Fig. 7 for six European countries and Fig. 8 for six Asian countries, respectively.

As we can see from Figs. 7 and 8, regardless of the geographical differences in the large-scale regions, it is extremely surprising to observe the essentially identical fractal features (i.e., hierarchy of structures) expressed by the multiple ripples, which are highlighted in blue segments, as shown in the β_0 curves as well as the multiple peaks in the β_1 curves for each of all the aforementioned 12 countries.

Despite the essential fractal features, there are still some obvious differences among the Betti curves of these countries, which can be summarized in three aspects as follows.

- 1) The numbers of the ripples or peaks for these countries are not entirely the same. For example, the number of ripples is 3 for France and Germany, and 2 for other ten countries. In addition, there seems to be no clear patterns in the number of ripples among the six Asian or European countries, which may imply that this parameter is not determined by the geographical position of the country. As indicated before, the number of ripples is closely associated with the hierarchical levels in the BS distributions, which are influenced by numerous historical, cultural, and

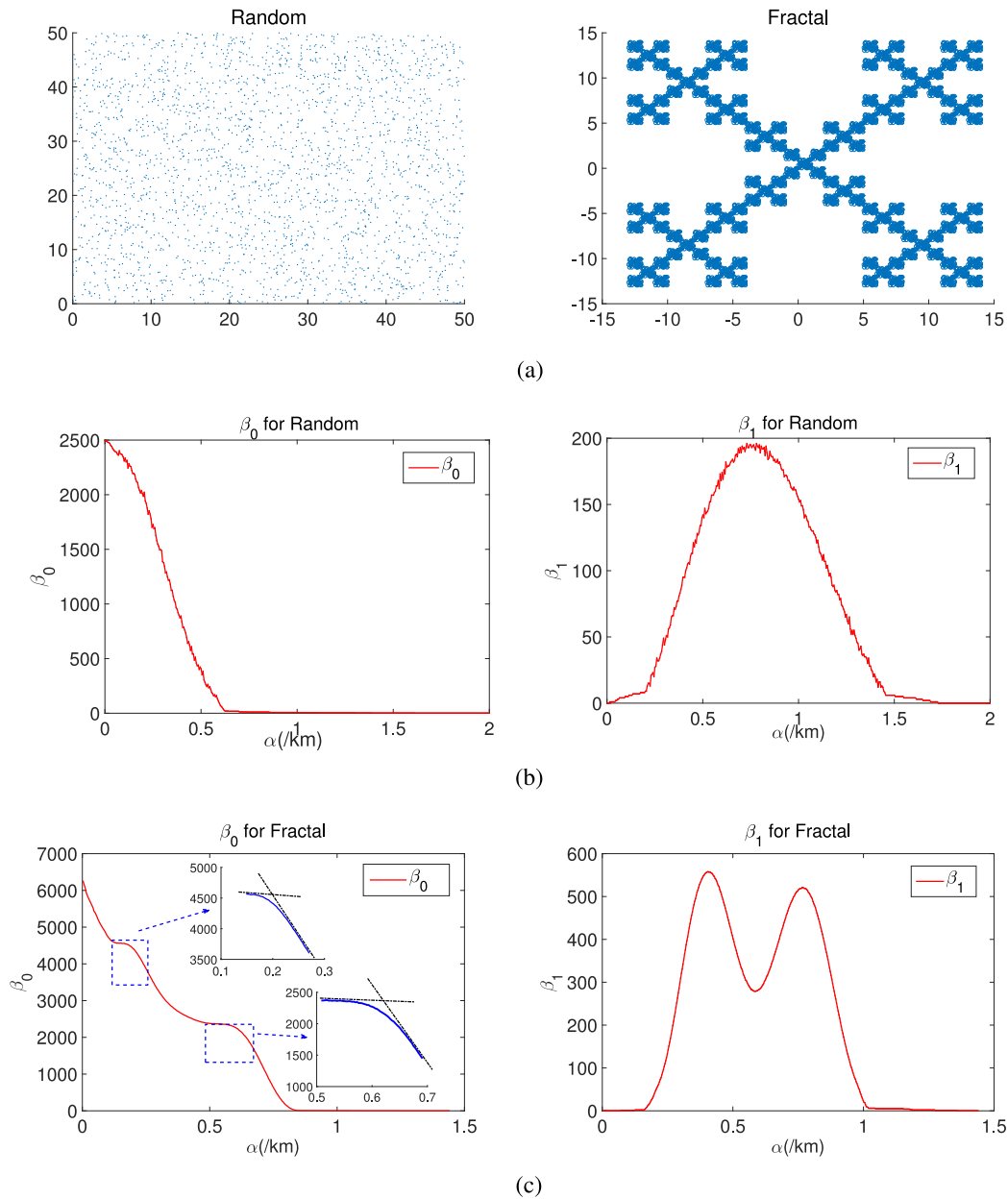


Fig. 6. Comparisons between the representative Betti curves of random and fractal point distributions. (a) Points deployment diagrams: (left) random; (right) fractal. (b) Betti curves for random: (left) β_0 ; (right) β_1 . (c) Betti curves for fractal: (left) β_0 ; (right) β_1 .

technological factors along the long evolution of these countries.

- 2) The amplitudes of the ripples or peaks are distinctive among these countries. For instance, the amplitude of the first β_1 peak of South Korea and Japan in Fig. 8(b) and (c) is around 850 and 11 500, respectively, which are considerably different even though the Betti curves for South Korea and Japan have pretty similar shapes. This parameter is related to the number of BSs in corresponding levels, which is affected by the total number of BSs of each country, and many other historical, cultural, and technological factors as well.
- 3) In addition, the ripples and peaks appear at completely different values of the scale parameter for each country, which are listed in Table III. It is noteworthy that the

ripples suggest the rapid gradient switch within a narrow range of, and the position of a ripple can be estimated according to the intersection of two straight lines with distinctive slopes, respectively, as shown in the first and third columns in Figs. 7 and 8. The positions are probably related to the area of the country, the density of BSs, and tightly associated to the unique developments of each country in historical, cultural, and technological aspects.

C. Fractal Features Based on the Hurst Coefficients

First, proposed by H. E. Hurst, the Hurst coefficient has recently gained its popularity in plenty of fields, especially in the finance fields as a result of Peter's work [45], [46]. As a measurement for fractality of data series, the Hurst coefficient usually

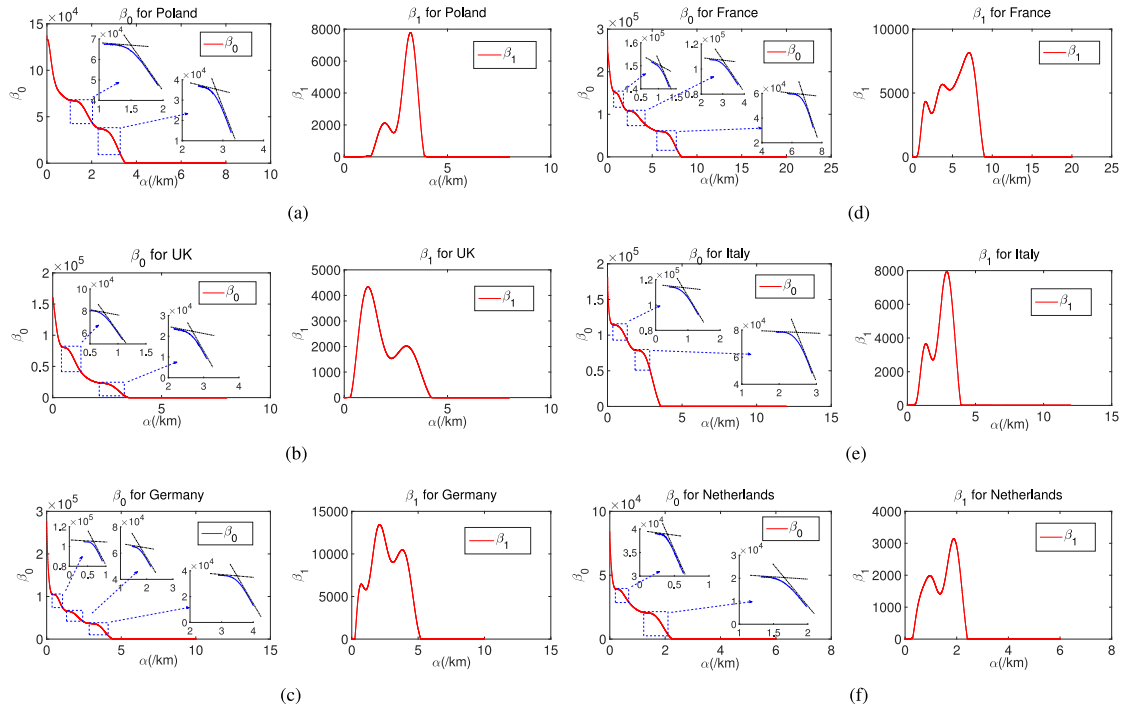


Fig. 7. Betti curves of the practical BSs distributions in European countries. (a) Poland. (b) UK. (c) Germany. (d) France. (e) Italy. (f) Netherlands.

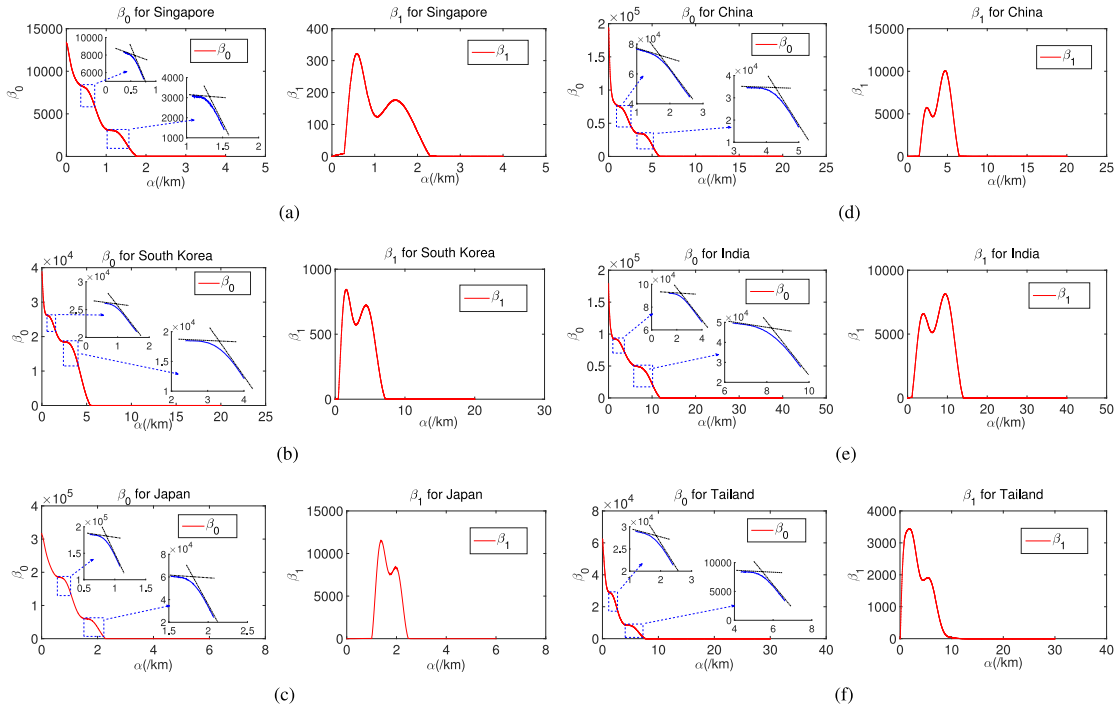


Fig. 8. Betti curves of the practical BSs distributions in Asian countries. (a) Singapore. (b) Korea. (c) Japan. (d) China. (e) India. (f) Thailand.

falls in the range from 0 to 1. In concrete, Hurst coefficient of 0.5 implies a completely random data series, while the indication of fractal features gets stronger as the value comes closer to 1 [47].

Among the various methods applied in the calculation of the Hurst coefficient, we take advantage of the rescaled range analysis (R/S), one of the most classical methods, in our works. Due to the space limitation, the framework of Hurst coefficient

computations is given in the Algorithm 1 below, and interested readers could refer to [48] for the details of the R/S method.

Actually, the length n of sub-series is variable, and it has been found that $(R/S)_n$ scales by power-law as n grows [48]

$$(R/S)_n = c \cdot n^H \quad (4)$$

TABLE III
POSITIONS OF THE RIPPLES AND PEAKS IN THE BETTI CURVES

State	Country	Index	β_0	β_1
Europe	Poland	1st	1.484	1.956
		2nd	2.816	3.208
	UK	1st	0.740	1.152
		2nd	2.644	3.012
	Germany	1st	0.640	0.710
		2nd	1.755	2.095
		3rd	3.485	3.800
	France	1st	1.090	1.640
		2nd	2.970	3.750
		3rd	6.780	7.090
Italy	1st	0.840	1.356	
	2nd	2.460	2.904	
Netherlands	1st	0.387	0.963	
	2nd	1.644	1.887	
Asia	Singapore	1st	0.572	0.580
		2nd	1.298	1.484
	South Korea	1st	0.950	1.580
		2nd	3.330	4.420
	Japan	1st	0.852	1.389
		2nd	1.818	1.971
	China	1st	1.670	2.430
		2nd	4.280	4.730
	Tailand	1st	1.845	1.875
		2nd	5.430	5.520
India	1st	2.360	3.940	
	2nd	8.200	9.460	

TABLE IV
HURST COEFFICIENTS FOR ALL THE 12 COUNTRIES

	Country	Hurst	Country	Hurst	
Europe	Poland	0.97978	Asia	Singapore	0.88466
	UK	0.98870		South Korea	0.98500
	Germany	0.97341		Japan	0.99275
	France	0.95323		China	0.91452
	Italy	0.97718		Tailand	0.96666
	Netherlands	0.98748		India	0.89700

where c is a constant, and the Hurst coefficient H can be estimated by the slope of the least-squares regression on logarithms of both sides in the above-mentioned equation.

In order to testify the fractal property in the cellular networks, the Hurst coefficients are computed for all the BSs in the cellular networks of all the selected countries. In this paper, an arbitrary center point is chosen randomly among all the location data of the BSs and a radius is specified first, so that a circle is formed given the center BS and the radius. Then, the distances between all the BSs within the circle and the center BS are calculated. In other words, the data series consist of a sequence of the distances between each BS and the center BS. Next, the Hurst coefficient is computed according to the data series in the way mentioned above. The similar process is performed a hundred times given different center points and radii, and the average Hurst coefficient is obtained finally. As indicated in Table IV, the fractal features are completely confirmed since all the Hurst coefficients are very close to 1.

Algorithm 1: The Framework of Hurst Coefficient Computations.

divide a data series $X = X_1, X_2, \dots, X_N$ of length N into A sub-series of the same length n
for each $a \in [1, A]$ **do**

$$\mu_a = \frac{1}{n} \sum_{i=(a-1)n+1}^{an} X_i,$$

// The mean value μ_a of the a -th sub-series.

$$Y_i = X_i - \mu_a, i = (a-1)n+1, (a-1)n+2, \dots, an.$$

// The mean adjusted sub-series Y .

$$Z_t = \sum_{i=(a-1)n+1}^t Y_i, t = (a-1)n+1, (a-1)n+2, \dots, an.$$

// The cumulative deviate series Z .

$$R_a = \max\{Z_{(a-1)n+1}, Z_{(a-1)n+2}, \dots, Z_{an}\} \\ - \min\{Z_{(a-1)n+1}, Z_{(a-1)n+2}, \dots, Z_{an}\}.$$

// The accumulated deviation R_a for the a -th sub-series.

$$S_a = \sqrt{\frac{1}{n} \sum_{i=(a-1)n+1}^{an} (X_i - \mu_a)^2}.$$

//The standard deviation series S_a for the a -th sub-series.

end for

$$(R/S)_n = \frac{1}{A} \sum_{a=1}^A R_a/S_a.$$

TABLE V
CANDIDATE DISTRIBUTIONS AND THEIR PDF EXPRESSIONS

Distributions	PDF
Poisson	$\frac{\lambda^k}{k!} e^{-\lambda}$
Weibull	$pqx^{q-1} e^{-px^q}$
Lognormal	$\frac{1}{\sqrt{2\pi}nx} e^{-\frac{(\ln x - m)^2}{2n^2}}$
Generalized Pareto(GP)	$\frac{1}{b} (1 + \frac{a}{b}x)^{-(1+\frac{1}{a})}$

V. CONSISTENT LOG-NORMAL DISTRIBUTION OF THE EULER CHARACTERISTICS

In this paper, based on Euler–Poincare Formula, the Euler Characteristics are obtained by subtracting β_1 from β_0 [4]. Obvious heavy-tail features can be observed from the curves of real probability density functions (PDFs), so several representative heavy-tail distributions and the widely used Poisson distribution are chosen as the candidate distributions for the fitness of real

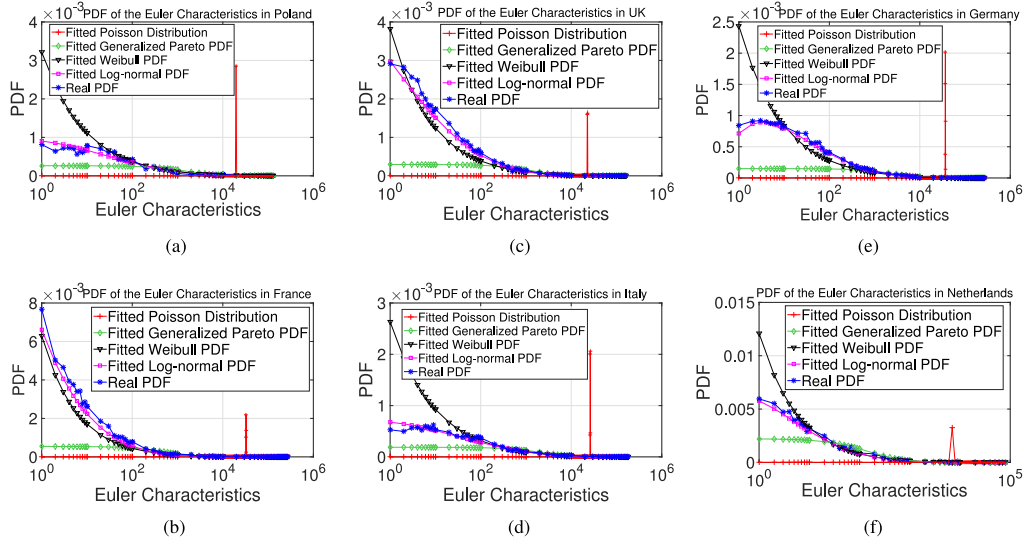


Fig. 9. Comparisons between the practical PDF and the fitted ones for European countries. (a) Poland. (b) France. (c) UK. (d) Italy. (e) Germany. (f) Netherlands.

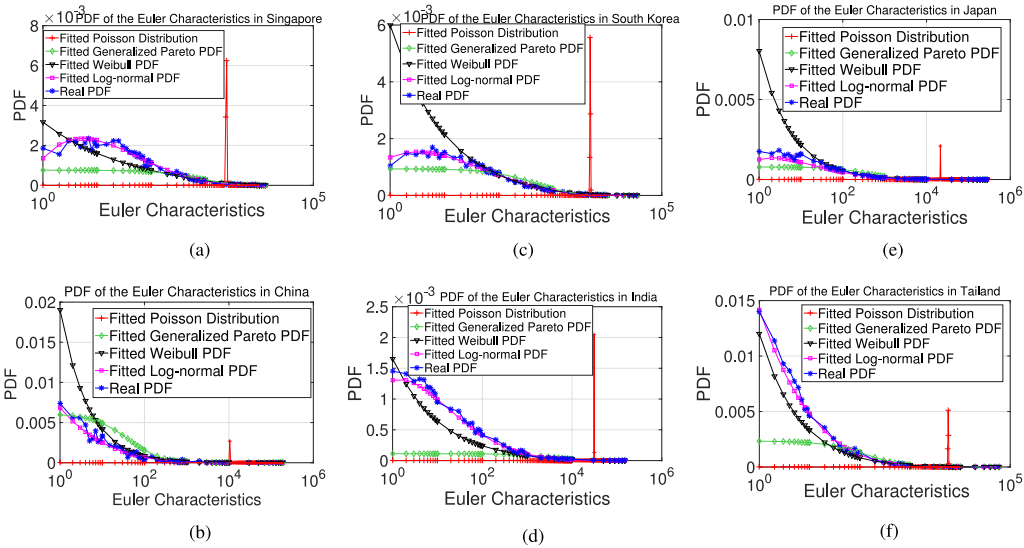


Fig. 10. Comparisons between the practical PDF and the fitted ones for Asian countries. (a) Singapore. (b) China. (c) South Korea. (d) India. (e) Japan. (f) Thailand.

PDF. The candidate distributions and their PDF expressions are listed in Table V.

During the process of data fitting, the Euler characteristics are assumed to comply with a specific statistical distribution to estimate the parameters, then an estimated PDF curve is generated to fit the given data. The comparisons between the practical PDF and the fitted ones are displayed in Fig. 9 for European countries and Fig. 10 for Asian ones, respectively.

As observed from the fitted curves in Figs. 9 and 10, for each European or Asian country, the log-normal distribution is clearly the closest one to the real PDF. Due to inevitable data deficiencies, the practical PDF curves, i.e., the blue curves in Figs. 9 and 10, are not completely smooth. For each country, the fitted log-normal PDF conforms to the shape and trend of the practical one to a great extent even if these two curves are not identically the same, while other three fitted PDFs, i.e., fitted Poisson,

Generalized Pareto, and Weibull PDFs, are apparently not even close to the practical PDF.

For the purpose of verifying the best match for the real PDFs, the root mean square error (RMSE) between each candidate distribution and the practical one is computed and listed in Table VI. As shown in Table VI, the RMSE between the log-normal distribution and the real PDF is also the smallest one for every country, which is almost one order of magnitude smaller than the other terms in the same row. In other words, the log-normal distribution is the best match for the PDF of the Euler characteristics for both European and Asian countries, from the perspective of either intuition or rigorous numerical analyses.

Therefore, a possibly surprising but well-founded conclusion can be drawn here: regardless of the geographical differences as well as the culture and historical factors, the Euler characteristics

TABLE VI
RMSE BETWEEN EACH CANDIDATE DISTRIBUTION AND THE PRACTICAL ONE

Distributions		Possion	Lognormal	Generalized _Pareto	Weibull
Country		($\times 10^{-4}$)	($\times 10^{-4}$)	($\times 10^{-4}$)	($\times 10^{-4}$)
Europe	Poland	1.23	0.07	0.12	0.23
	UK	1.09	0.11	0.74	0.42
	Germany	0.75	0.02	0.11	0.16
	France	0.84	0.08	0.28	0.12
	Italy	0.99	0.05	0.19	0.29
	Netherlands	2.15	0.17	0.37	0.30
Asia	Singapore	3.72	0.14	0.96	0.69
	South Korea	3.30	0.09	0.26	0.38
	Japan	0.81	0.08	0.20	0.17
	China	1.28	0.08	0.43	0.40
	Tailand	2.84	0.11	0.89	0.47
	India	0.98	0.05	0.18	0.11

of either Asian or European countries completely comply with the log-normal distribution.

VI. CONCLUSION AND FUTURE WORK

In this paper, the algebraic geometric tools, i.e., α -Shapes, Betti numbers, and Euler characteristics, have been exploited to discover the intrinsic topological characteristics from the real BS location data of various Asian and European countries. First of all, fractal phenomenon has been confirmed within the BS configurations for either Asian or European countries in terms of both Betti numbers and Hurst coefficients. Second, the log-normal distribution has been proven to provide the best fitness to the PDFs of the Euler characteristics among typical distribution candidates in regard to the practical BS deployments in the cellular networks.

Nevertheless, despite all the topological findings mentioned above, there are still some challenging issues to be worked out in the future. For instance, what are the definitive factors for the α values of the ripples and peaks in the Betti curves? What is the intrinsic meaning of the number of levels indicated by the number of ripples or peaks? And how to apply the log-normal distribution of the Euler characteristics to the design of BSs deployments? What are the essential reasons behind the topological features shown in the figures? We will investigate all of these problems as our future works.

REFERENCES

- [1] J. Kibida, B. Galkin, and L. A. Dasilva, "Modelling multi-operator base station deployment patterns in cellular networks," *IEEE Trans. Mobile Comput.*, vol. 15, no. 12, pp. 3087–3099, Dec. 2016.
- [2] R. V. D. Weygaert, G. Vegter, E. Platen, B. Eldering, and N. Kruithof, "Alpha shape topology of the cosmic web," in *Proc. Int. Symp. Voronoi Diagrams Sci. Eng.*, Quebec, QC, Canada, Jun. 2010, pp. 224–234.
- [3] P. Pranav *et al.*, "The topology of the cosmic web in terms of persistent Betti numbers," *Monthly Notices Roy. Astronomical Soc.*, vol. 4, no. 465, pp. 4281–4310, Mar. 2017.
- [4] R. V. D. Weygaert *et al.*, *Alpha, Betti, and the Megaparsec Universe: On the Topology of the Cosmic Web*. Berlin, Germany: Springer, 2011.
- [5] V. D. Silva and R. Ghrist, "Coverage in sensor networks via persistent homology," *Algebr. Geometric Topology*, vol. 7, no. 1, pp. 339–358, Apr. 2007.
- [6] Y. Chen, R. Li, Z. Zhao, and H. Zhang, "Study on base station topology in cellular networks: Take advantage of alpha shapes, Betti numbers, and Euler characteristics," Aug. 2018, arXiv:1808.07356v1.
- [7] Y. Chen, R. Li, Z. Zhao, and H. Zhang, "Fundamentals on base stations in cellular networks from the perspective of algebraic topology," *IEEE Wireless Commun. Lett.*, vol. 8, no. 2, pp. 612–615, Apr. 2019.
- [8] M. Ericson, "Total network base station energy cost vs. deployment," in *Proc. IEEE 73rd Veh. Technol. Conf.*, Yokohama, Japan, May 2011, pp. 1–5.
- [9] Y. Lin, Q. Wu, X. Cai, and N. S. V. Rao, "Optimizing base station deployment in wireless sensor networks under one-hop and multi-hop communication models," in *Proc. 15th Int. Conf. Parallel Distrib. Syst.*, Shenzhen, China, Dec. 2009, pp. 96–103.
- [10] J. Liu, T. Kou, Q. Chen, and H. D. Sherali, "Femtocell base station deployment in commercial buildings: A global optimization approach," *IEEE J. Sel. Areas Commun.*, vol. 30, no. 3, pp. 652–663, Apr. 2012.
- [11] Y. Wu and Z. Niu, "Energy efficient base station deployment in green cellular networks with traffic variations," in *Proc. 1st IEEE Int. Conf. Commun. China*, Beijing, China, Aug. 2012, pp. 399–404.
- [12] C. C. Coskun and E. Ayanoglu, "A greedy algorithm for energy-efficient base station deployment in heterogeneous networks," in *Proc. IEEE Int. Conf. Commun.*, London, U.K., Jun. 2015, pp. 7–12.
- [13] S. Istv and P. Fazekas, "An algorithm for automatic base station placement in cellular network deployment," in *Proc. Meeting Eur. Netw. Universities Companies Inf. Commun. Eng.*, Trondheim, Norway, Jun. 2010, pp. 21–30.
- [14] S. Mahmud, H. Wu, and J. Xue, "Efficient energy balancing aware multiple base station deployment for WSNs," in *Proc. 8th Eur. Conf. Wireless Sensor Netw.*, Bonn, Germany, Feb. 2011, pp. 179–194.
- [15] Y. Zhou, R. Li, Z. Zhao, X. Zhou, and H. Zhang, "On the α -stable distribution of base stations in cellular networks," *IEEE Commun. Lett.*, vol. 19, no. 10, pp. 1750–1753, Oct. 2015.
- [16] Y. Zhou *et al.*, "Large-scale spatial distribution identification of base stations in cellular networks," *IEEE Access*, vol. 3, pp. 2987–2999, Dec. 2015.
- [17] M. Li, Z. Zhao, Y. Zhou, X. Chen, and H. Zhang, "On the dependence between base stations deployment and traffic spatial distribution in cellular networks," in *Proc. 23rd Int. Conf. Telecommun.*, Thessaloniki, Greece, May 2016, pp. 1–5.
- [18] L. Chiaraviglio, F. Cuomo, M. Maisto, and A. Gigli, "What is the best spatial distribution to model base station density? A deep dive into two European mobile networks," *IEEE Access*, vol. 4, pp. 1434–1443, 2016.
- [19] Z. Zhao, M. Li, R. Li, and Y. Zhou, "Temporal-spatial distribution nature of traffic and base stations in cellular networks," *IET Commun.*, vol. 11, no. 16, pp. 2410–2416, 2017.
- [20] S. Athanassopoulos, C. Kaklamanis, P. Katsikouli, and E. Papaioannou, "Cellular automata for topology control in wireless sensor networks," in *Proc. 16th IEEE Mediterranean Electrotechnical Conf.*, Hammamet, Tunisia, Mar. 2012, pp. 212–215.
- [21] T. Kwon and M. S. Lee, "Random multicell topology adjustment for green-cellular networks," in *Proc. IEEE Int. Conf. Commun.*, London, U.K., Jun. 2015, pp. 204–209.
- [22] N. Xiang, W. Li, L. Feng, F. Zhou, and P. Yu, "Topology-aware base station energy-saving mechanism in wireless cellular networks," in *Proc. IFIP/IEEE Int. Symp. Integr. Netw. Manage.*, Ottawa, ON, Canada, May 2015, pp. 538–544.
- [23] R. Torrea-Duran, M. M. Cspedes, J. Plata-Chaves, L. Vandendorpe, and M. Moonen, "Topology-aware space-time network coding in cellular networks," *IEEE Access*, vol. 6, pp. 7565–7578, 2018.
- [24] A. Dharmaraj, H. Li, N. Weragama, and D. P. Agrawal, "Distributed topology-based resource allocation for a femtocell-based cellular network," in *Proc. 13th Int. Conf. Comput. Sci. Appl.*, Ho Chi Minh City, Vietnam, Jun. 2013, pp. 13–18.
- [25] R. Li, Z. Zhao, Y. Zhong, C. Qi, and H. Zhang, "The stochastic geometry analyses of cellular networks with α -stable self-similarity," *IEEE Trans. Commun.*, vol. 67, no. 3, pp. 2487–2503, Mar. 2019.
- [26] X. Ge, X. Tian, Y. Qiu, G. Mao, and T. Han, "Small cell networks with fractal coverage characteristics," *IEEE Trans. Commun.*, vol. 66, no. 11, pp. 5457–5469, Nov. 2018.

- [27] H. Wagner, P. Dotko, and M. Mrozek, "Computational topology in text mining," in *Proc. 4th Int. Conf. Comput. Topology Image Context*, Bertinoro, Italy, May 2012, pp. 68–78.
- [28] A. J. Zomorodian, *Topology For Computing* (Series Cambridge Monographs on Applied and Computational Mathematics). Cambridge, U.K.: Cambridge Univ. Press, 2005.
- [29] D. E. Knuth, *The Art of Computer Programming*. Reading, MA, USA: Addison-Wesley, 1973.
- [30] W. Zhou and H. Yan, *A Discriminatory Function For Prediction of Protein-DNA Interactions Based on Alpha Shape Modeling*. London, U.K.: Oxford Univ. Press, 2010.
- [31] J. A. Wilson, A. Bender, T. Kaya, and P. A. Clemons, "Alpha shapes applied to molecular shape characterization exhibit novel properties compared to established shape descriptors," *J. Chem. Inf. Model.*, vol. 49, no. 10, pp. 2231–2241, 2009.
- [32] J. Liang and E. Al, "Analytical shape computation of macromolecules: I. Molecular area and volume through alpha shape," *Proteins-Struct. Function Bioinf.*, vol. 33, no. 1, pp. 1–17, 1998.
- [33] L. Mu and R. Liu, "A heuristic alpha-shape based clustering method for ranked radial pattern data," *Appl. Geography*, vol. 31, no. 2, pp. 621–630, 2011.
- [34] M. Fayed and H. T. Mouftah, "Localised alpha-shape computations for boundary recognition in sensor networks," *Ad Hoc Netw.*, vol. 7, no. 6, pp. 1259–1269, 2009.
- [35] R. Ohbuchi and T. Takei, "Shape-similarity comparison of 3D models using alpha shapes," in *Proc. 11th Pacific Conf. Comput. Graph. Appl.*, Oct. 2003, pp. 293–302.
- [36] H. Edelsbrunner, "Alpha shapes—A survey," *Tessellations Sci.*, vol. 6, pp. 1–25, 2010.
- [37] W. Zhou and H. Yan, "Alpha shape and Delaunay triangulation in studies of protein-related interactions," *Briefings Bioinf.*, vol. 15, no. 1, pp. 54–64, Nov. 2012.
- [38] M. Ulm, P. Widhalm, and N. Brandle, "Characterization of mobile phone localization errors with opencellid data," in *Proc. Int. Conf. Adv. Logistics Transport*, Valenciennes, France, May 2015, pp. 100–104.
- [39] C. Yuan, Z. Zhao, R. Li, M. Li, and H. Zhang, "The emergence of scaling law, fractal patterns, and small-world in wireless networks," *IEEE Access*, vol. 5, pp. 3121–3130, 2017.
- [40] X. Ge *et al.*, "Wireless fractal cellular networks," *IEEE Wireless Commun.*, vol. 23, no. 5, pp. 110–119, Oct. 2016.
- [41] Y. Hao, M. Chen, L. Hu, J. Song, M. Volk, and I. Humar, "Wireless fractal ultra-dense cellular networks," *Sensors*, vol. 17, no. 4, pp. 8411–8417, Apr. 2017.
- [42] S. H. Strogatz, "Complex systems: Romanesque networks," *Nature*, vol. 433, no. 7024, pp. 365–366, Jan. 2005.
- [43] C. Song, S. Havlin, and H. A. Makse, "Self-similarity of complex networks," *Nature*, vol. 433, no. 7024, pp. 392–395, Jan. 2005.
- [44] D. Benhaïem, M. Joyce, and B. Marcos, "Self-similarity and stable clustering in a family of scale-free cosmologies," *Monthly Notices Roy. Astronomical Soc.*, vol. 443, no. 3, pp. 2126–2153, Jul. 2014.
- [45] T. A. Noll, "Chaos and order in the capital markets: A new view of cycles, prices, and market volatility," *J. Finance*, vol. 48, no. 5, pp. 2041–2328, 1993.
- [46] E. E. Peters, "Fractal market analysis: Applying chaos theory to investment and economics," *Chaos Theory*, vol. 34, no. 2, pp. 343–345, 1994.
- [47] T. Gneiting and M. Schlather, "Stochastic models which separate fractal dimension and Hurst effect," *Soc. Ind. Appl. Math. Rev.*, vol. 46, no. 2, pp. 269–282, 2001.
- [48] M. Fernández-Martínez, M. A. Sánchez-Granero, J. E. T. Segovia, and I. M. Román-Sánchez, "An accurate algorithm to calculate the Hurst exponent of self-similar processes," *Phys. Lett. A*, vol. 378, no. 32/33, pp. 2355–2362, 2014.



Ying Chen received the B.S. degree from the College of Information and Engineering, Southeast University, Nanjing, China, in 2016. She is currently working toward the Ph.D. degree with the College of Information Science and Electrical Engineering, Zhejiang University, Hangzhou, China.

Her research interests include the information capacity in complex networks, algebraic topology in wireless cellular networks, and deep neural networks.



Rongpeng Li received the B.E. degree from Xidian University, Xi'an, China, in 2010, and the Ph.D. degree from Zhejiang University, Hangzhou, China, in 2015, both as excellent graduates.

From 2015 to 2016, he was a Research Engineer with the Wireless Communication Laboratory, Huawei Technologies Co. Ltd., Shanghai, China. He returned to academia, in 2016, initially as a Postdoctoral Researcher with the College of Computer Science and Technologies, Zhejiang University, which is sponsored by the National Postdoctoral Program for Innovative Talents. He is currently an Assistant Professor with the College of Information Science and Electronic Engineering, Zhejiang University, Hangzhou, China. He has authored/coauthored several papers in the related fields. His research interests currently focus on reinforcement learning, data mining, and all broad-sense network problems (e.g., resource management and security).

Dr. Li serves as an Editor for *China Communications*.



Zhifeng Zhao received the bachelor's degree in computer science, the master's degree in communication and information system, and the Ph.D. degree in communication and information system from the PLA University of Science and Technology, Nanjing, China, in 1996, 1999, and 2002, respectively.

From 2002 to 2004, he was a Postdoctoral Researcher with Zhejiang University, Hangzhou, China, where his works were focused on multimedia next-generation networks and soft-switch technology for energy efficiency. From 2005 to 2006, he was a Senior Researcher with the People's Liberation Army University of Science and Technology, where he performed research and development on advanced energy-efficient wireless router, ad hoc network simulator, and cognitive mesh networking test bed. He is currently the Director of the Research Development Department, Zhejiang Lab, China. He is also with Zhejiang University. His research interests include cognitive radio, wireless multi-hop networks (ad Hoc, mesh, and WSN), wireless multimedia networks, and green communications.

Dr. Zhao is the Symposium Co-Chair of the China Com 2009 and 2010. He is the Technical Program Committee (TPC) Co-Chair of the IEEE 10th IEEE International Symposium on Communication and Information Technology (ISCT) 2010.



Honggang Zhang was the International Chair Professor of Excellence with the Université Européenne de Bretagne and Supélec, France. He is currently a Full Professor with the College of Information Science and Electronic Engineering, Zhejiang University, Hangzhou, China. He is also an Honorary Visiting Professor with the University of York, York, U.K. He was a co-author and an Editor of three books *Cognitive Communications-Distributed Artificial Intelligence* (Wiley), *Regulatory Policy and Economics, Implementation* (Wiley), and *Green Communications: Theoretical Fundamentals, Algorithms, and Applications* (CRC Press), respectively. He is also active in the research on cognitive radio and green communications.

Dr. Zhang served as the Chair for the Technical Committee on Cognitive Networks of the IEEE Communications Society, from 2011 to 2012. He was a leading Guest Editor of the IEEE COMMUNICATIONS MAGAZINE-Special Issues on Green Communications as well as a Series-Editor of the IEEE COMMUNICATIONS MAGAZINE for its Green Communications and Computing Networks Series. He is the Associate Editor-in-Chief of *China Communications*.